Journal of Peptide Science
J. Pept. Sci. 2008; **14**: 661–669
Published online 12 November 2007 in Wiley InterScience (www.interscience.wiley.com). DOI: 10.1002/psc.960

JOURNAL OF PEPTIDE SCIENCE

Study of the mechanism of action of anoplin, a helical antimicrobial decapeptide with ion channel-like activity, and the role of the amidated *C*-terminus

MARCIA PEREZ DOS SANTOS CABRERA,[a]* MANOEL ARCISIO-MIRANDA,[a] SABRINA THAIS BROGGIO COSTA,[b] KATSUHIRO KONNO,[c] JOSÉ ROBERTO RUGGIERO,[b] JOAQUIM PROCOPIO[a] and JOÃO RUGGIERO NETO[b]

[a] USP - University of São Paulo, Department of Physiology and Biophysics, Biomedical Sciences Institute, Av. Prof. Lineu Prestes, 1524, 05508-900 São Paulo, SP, Brazil
[b] UNESP - São Paulo State University, Department of Physics, IBILCE, S. José do Rio Preto, SP, Brazil
[c] CAT CEPID, Center for Applied Toxinology, Instituto Butantan, São Paulo, SP, Brazil

Received 30 July 2007; *Revised 11 September 2007*; *Accepted 19 September 2007*

Abstract: Anoplin, an antimicrobial, helical decapeptide from wasp venom, looses its biological activities by mere deamidation of its *C*-terminus. Secondary structure determination, by circular dichroism spectroscopy in amphipathic environments, and lytic activity in zwitterionic and anionic vesicles showed quite similar results for the amidated and the carboxylated forms of the peptide. The deamidation of the *C*-terminus introduced a negative charge at an all-positive charged peptide, causing a loss of amphipathicity, as indicated by molecular dynamics simulations in TFE/water mixtures and this subtle modification in a peptide's primary structure disturbed the interaction with bilayers and biological membranes. Although being poorly lytic, the amidated form, but not the carboxylated, presented ion channel-like activity on anionic bilayers with a well-defined conductance step; at approximately the same concentration it showed antimicrobial activity. The pores remain open at *trans*-negative potentials, preferentially conducting cations, and this situation is equivalent to the interaction of the peptide with bacterial membranes that also maintain a high negative potential inside. Copyright © 2007 European Peptide Society and John Wiley & Sons, Ltd.

Keywords: anoplin; antimicrobial peptide; lytic activity; ion channel; pore activity; peptide-membrane interactions; molecular dynamics

INTRODUCTION

The decapeptide anoplin (ANP), GLLKRIKTLL, is among the smallest naturally occurring antimicrobial peptides. The *C*-terminus amidated form (ANP–NH_2) isolated from the venom sac of pompilid wasp's *Anoplius samariensis* presents antimicrobial and mast cell degranulating activities, and is not hemolytic [1]. It is water-soluble because of the presence of four-polar residues, which confer a highly hydrophilic character, −0.113 mean hydrophobicity, according to Eisenberg's consensus scale [2]. The interaction with amphipathic environments, like TFE/water mixtures, or with anisotropic media, as SDS micelles or anionic vesicles, induces α-helical conformations, as indicated by CD spectra, and gives rise to its amphiphilic character. However, in the presence of zwitterionic phosphatidylcholine vesicles the unordered structure is the most frequent [1]. Previous results with ANP-NH_2 [1,3] have also suggested that besides its net charge, the primary sequence and probably the secondary structure, adopted upon contact with biological membranes, might be very important to modulate its biological activities.

N- and *C*-termini features are relatively more important for the helical content and biological activities of short-chain peptides than for those with longer chains [4–6]. It has been shown, in the last 10 years, that the bilayer permeabilization efficiency of antimicrobial peptides is, in general, correlated with some physicochemical characteristics [7]: net charge, hydrophobicity, helicity, hydrophobic moment, and the angle subtended by the polar face; most of them influenced by the helix macrodipole and *N*- and *C*-termini characteristics. Considering that the biological activity of antimicrobial peptides is targeted to the membrane lipids [4,8,9], understanding these interactions is an important step in the search for new sources in antibiotic therapy [10]. Additionally, short sequences are useful as tools for investigating mechanisms of action [11], and can be compared to homologous sequences of membrane protein [12] or signal peptides for their conformational and interactions similarities [13]. As an example, searching ANP sequence in FASTA data bank [14], it has been found out, among others, an interesting 7-amino acid overlap (1–7 : 59–65) with the *C*-terminus of LAMBD

Abbreviations: CD, Circular Dichroism spectroscopy; MD, Molecular Dynamics; LUVs, large unilamellar vesicles; TFE, trifluoroethanol; CF, carboxyfluorescein; PC, L-α-phosphatidylcholine; PG, L-α-phosphatidyl-DL-glycerol; CL, cardiolipin.

*Correspondence to: Marcia Perez Dos Santos Cabrera, USP - University of São Paulo, Department of Physiology and Biophysics, Biomedical Sciences Institute, Av. Prof. Lineu Prestes, 1524, 05508-900 São Paulo, SP, Brazil; e-mail: cabrera.marcia@gmail.com

Excisionase. This is a 73-residues enzyme that plays a key role in the mechanism of excisive recombination of bacteriophages, by reorienting the recombination directionality. Mutations in this segment had marked effects on the interactions of the enzyme and these have been attributed to changes in the required structural motif [15].

Other solitary wasp venom peptides like wild types Eumenitin [11] and Decoralin [16] and synthetic EMP-AF1 [17] are carboxylated at the *C*-terminus and present significantly reduced hemolytic and mast cell degranulating activities, in comparison to other mastoparan-like peptides with amidated *C*-terminus. An ANP analog with a carboxylated *C*-terminus, ANP-OH, has been synthesized, to further investigate the modulating role of this modification to the biological activity and the differences on their mechanism of action. This has been accomplished in two steps: first, considering that membrane permeabilization is related to antimicrobial activity and that the outer leaflet of the bacterial membrane is, in general, negatively charged, while in mammals it is electrically neutral [18–20], the lytic activity on charged and noncharged vesicles, in dye leakage experiments, and the channel-like activity in anionic (azolectin) planar lipid bilayers have been determined. Second, MD simulations have been carried out in TFE/water mixture, a noncharged environment, with amphipathic characteristics, to prospect information regarding the molecular differences between these structures.

MATERIALS AND METHODS

Peptide Synthesis and Purification

ANP-NH_2 and ANP-OH were synthesized as described by Konno *et al.* [1], by step-wise solid-phase method, using *N*-9-fluorophenylmethoxycarbonyl (Fmoc) strategy on a Shimadzu PSSM-8 peptide synthesizer (Shimadzu, Kyoto, Japan). The crude products were purified by reverse-phase HPLC, and the homogeneity and sequence were accessed by analytical HPLC and mass spectrometry (MALDI-TOF-MS and ESI-MS).

Vesicle Preparation

Lipids and CF were purchased from Sigma-Aldrich (St Louis, MO). The following lipid films were prepared: zwitterionic, composed of pure PC; anionic, made up with pure azolectin, or lipid mixtures made of PC and either PG or CL at the following molar ratios: PC : PG 70 : 30 (PCPG 7030), PC : CL 70 : 30 (PCCL 7030) and PC : CL 40 : 60 (PCCL 4060). LUVs for dye leakage measurements have been prepared according to general procedures from the literature [13,21] with modifications as described elsewhere [5]. In short, chloroform solutions of the chosen lipids were evaporated under N_2 flow, rendering homogeneous films on round bottom flasks that were further dried under vacuum for at least 3 h. These films were hydrated with Tris/HCl 10 mM, 1mM Na_2EDTA, containing 25 mM CF, pH 7.5, for fluorescence experiments, and vortex mixed. LUVs were obtained after 5-min sonication, in an ice/water bath; titanium debris was removed by centrifugation. Vesicles have been submitted to 11 extrusions through two stacked 200 nm polycarbonate membranes and filtered through a Sephadex G25M gel column (Amercham Pharmacia, Uppsala, Sweden) to separate dye-entrapped LUV from free dye. They have been used within 48 h of preparation.

Dye Leakage

A volume of fresh LUV suspension was injected into a cuvette containing magnetically stirred peptide solutions either at 5.0 or at 20 μM, to give a final volume of 1.0 ml. These peptide concentrations cover the range of interest as determined in previous antimicrobial activity tests [1,3]. CF release from the vesicles was monitored at 520 nm (excited at 490 nm) on a Hitachi Fluorometer F4500 (Tokio, Japan) by measuring the decrease in self-quenching at 25 °C. Fluorescence intensity at 100% leakage (F_{100}) is determined by adding 10 μl of 10% Triton X-100 solution. Percent of dye leakage was determined after regular time intervals and calculated as $100 \times (F - F_0)/(F_{100} - F_0)$, where F is the measured fluorescence intensity and F_0 corresponds to the fluorescent intensity of intact LUV. This 100% leakage fluorescence has been corrected for the corresponding dilution factor.

Planar Lipid Bilayer Preparation and Single-channel Measurements and Analysis

Buffer for these experiments was Tris/HCl 10 mM plus 150 mM KCl at pH 7.5. Membranes were formed from a mixture of azolectin (Sigma-Aldrich, St Louis, MO) in *n*-decane (25 mg/l), according to the original method of Mueller [22]. A cylindrical glass cup having a 0.2–0.5 mm hole is coupled to an acrylic chamber; the cup separated two compartments, each filled with 5 ml buffer, and designated *cis* (front chamber, held at ground), and *trans* (rear chamber, connected to the probe). Electrical access to the baths was through a pair of Ag/AgCl electrodes.

Optical reflectance, resistance, and capacitance indicated the formation of planar lipid bilayers. To the *cis* compartment, 20 μl ANP-NH_2 or 25 μl ANP-OH stock solutions (0.9 mM) were added and stirred for 3 min using a stream of obliquely directed air over the bath surface. After a few minutes of equilibration, -50 mV potential was applied to the *trans* compartment in order to monitor the initial channel activity. Afterwards the *trans* side was clamped to a range of potentials and single-channel activity was recorded. The sign of the membrane potential refers to the *trans* compartment. The transmembrane current (I_m), under different clamping potentials (V_{clamp}), was monitored using a patch-clamp amplifier (Dagan 8900) configured in voltage-clamp mode. Membrane conductance (G_m) was obtained as $G_m = I_m/V_{clamp}$. Data were acquired using the Axotape 2.0.2 software and analyzed with AxoScope 8.0 (Axon Instruments); WinEDR (Strathclyde Electrophysiology Software package) was employed in the recordings of single channel events that allowed a statistical analysis.

The selectivity of the ion-channel was determined by measuring the open-circuit (spontaneous) transmembrane voltage under a KCl concentration gradient imposed across the membrane. The open-circuit voltage was monitored

DOI: 10.1002/psc

continuously by the patch-clamp amplifier configured in current-clamp mode. An excess peptide added in the *cis* side raised significantly the membrane conductance; afterwards, successive 100 μl aliquots of 2M KCl were added to the *cis* side under stirring. The total volume in the compartment was kept constant by taking out identical volumes of solution from a different bath corner, after the addition of each aliquot. The open-circuit voltage (V_{total}) was monitored continuously until a stable transmembrane voltage of 30–40 mV was obtained. Then the membrane was broken, and the voltage reading immediately recorded (V_{break}) was taken as the electrode asymmetry voltage. The open-circuit transmembrane voltage (V_{memb}) was given by $V_{memb} = V_{total} - V_{break}$.

Room temperature was 25 ± 2 °C throughout the measurements. The data were collected from a minimum of three experiments.

CD Spectroscopy Experiments

For both peptides, ANP-NH_2, and ANP-OH, CD spectra were obtained at 20 μM, pH 7.5, in TFE/buffer mixture (40% v/v) and buffered SDS solution (8 mM), above critical micellar concentration. To minimize noise-to-signal ratio and to provide similar conditions among CD, dye leakage, and single channel experiments, the buffer used was 5 mM Tris/H_3BO_3 with 0.5 mM EDTA and 150 mM NaF. CD spectra were recorded from 260 to 197 nm with a Jasco-710 spectropolarimeter (JASCO International Co. Ltd., Tokyo, Japan) which was routinely calibrated at 290.5 nm using *d*-10-camphorsulfonic acid solution. Spectra were acquired at 25 °C using 0.5-cm path length cell, averaged over six scans, at a scan speed of 20 nm/min, bandwidth of 1.0 nm, 0.5 s response, and 0.1 nm resolution. Following baseline correction, the observed ellipticity, θ (mdeg) was converted to mean-residue ellipticity $[\Theta]$ (deg cm^2/dmol), using the relationship $[\Theta] = 100\theta/(lcn)$ where '*l*' is the path length in centimeters, '*c*' is peptide milimolar concentration, and '*n*' the number of peptide residues.

MD Simulations

MD simulations of the peptides were carried out in a triclinic box containing TFE and water, corresponding approximately to a mixture of 30 : 70% (v/v) TFE : water. The system consisted of 205 TFE molecules, 1902 water molecules, and 4 chlorine (Cl^-) counterions, which neutralize the 4 positive charges in ANP-NH_2, and 3 Cl^- counterions, to neutralize ANP-OH net charge. In both the cases, the *N*-termini were treated as a positively charged group (NH_3^+); ANP-OH *C*-terminus was treated as a negatively charged carboxylated group (COO^-). The calculations were carried out using GROMOS 96 force field [23]; the Simple Point Charge model [24] was used for water molecules; for TFE molecules, the model and simulation conditions were applied as proposed by Fioroni *et al.* [25]. System optimization was carried out in 8000-steps conjugate gradient and a steepest descent cycle was performed every 500 steps. Position restriction dynamics for solvent and ions relaxation ran for 1 ns, with a 2-fs-time step for the integration of the equations of motion. After the removal of the constraints, the systems were submitted to 8 ns MD simulations. Periodic boundary conditions have been imposed to the system simulations with a cutoff radius of 1.4 nm. The LINCS [26] algorithm was used to constraint all bond lengths and SETTLE [27] to constraint water geometry. Simulations ran in the canonical ensemble (*n*, *P*, *T*) 300 K and 1 atm. Temperature and pressure were modulated using coupling techniques [28] with coupling and isothermal compressibility constants of 0.01 ps (solvent and peptide) and 6.5×10^{-5} bar^{-1}, respectively. Long-range electrostatic interactions were treated using Particle Mesh Ewald method [29]. For Lennard–Jones interactions the cutoff radius was 1.4 nm. The atomic positions were recorded every 1.0 ps throughout each trajectory. MD calculations and trajectory analysis were made using the facilities of the GROMACS package [30].

The strategy for the MD studies on ANP-NH_2 and its analog in TFE/water mixture (30 : 70 v/v) was to use the ideal α-helix of the amidated form as the starting structure. Two MD simulations of 8 ns have been carried out: first with the amidated *C*-terminus and in the second, the amide *C*-terminus group has been taken out, the compound remaining as a negatively charged carboxyl group.

RESULTS

ANP-OH has been tested in parallel with ANP-NH_2 for its biological activities, according to the procedures described in detail by Konno *et al.* [1]. Like its parent analog, ANP-OH has no hemolytic activity and the antimicrobial and mast cell degranulation activities were drastically reduced by deamidation. ANP-OH minimal inhibitory concentrations (MIC) increased above 100 μg/ml (~88 μM) in relation to the values obtained with ANP-NH_2 [1] against all tested microorganisms. An MIC increase was also observed for an analog truncated at residue Leu10 [3].

Leakage Experiments

The membrane permeabilization activity induced by ANP-NH_2 and ANP-OH was investigated through the release of CF from zwitterionic PC, and from the anionic PCPG 7030, PCCL (7030 and 4060) and azolectin LUV. Varying the phospholipid composition in this way intended to assess the influence of the anionic charge density and of the elastic properties of the bilayers, as well as to correlate these results with those of the ion channel-like activity. CL, a dimeric form of phosphatidylglycerol, has four acyl chains and two negative charges, one at each phosphate group. CL imposes negative curvature strain to bilayers and increases their compressibility modulii [31].

Both peptides at 5 μM and until 20 min contact time induced less than 10% CF release from PC and from all anionic vesicles tested (data not shown). Even when the peptide concentration was increased to 10 μM for PC vesicles and 20 μM for anionic vesicles, the dye-released fraction did not increase significantly within 5 min, as displayed in Figure 1 (hatched bars). In azolectin LUV, ANP-NH_2, and ANP-OH, concentration

DOI: 10.1002/psc

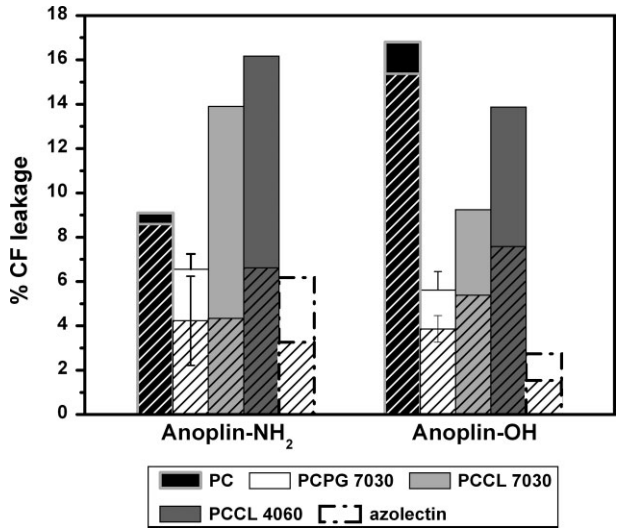

Figure 1 Percentage CF leakage induced by ANP-NH2 and ANP-OH in vesicles of different composition. On zwitterionic PC vesicles at 10 μM concentration, on anionic PCPG 7030, PCCL 7030, and PCCL 4060 vesicles at 20 μM and on azolectin vesicles at 30 μM. Lip/Pep ratio varied from 15 to 5. Contact time of 5 min shown in hatched bars and 20 min contact time with no pattern. Error bars are shown for both peptides with PCPG 7030 vesicles.

has been raised till 30 μM and the maximum leakage observed was 6%. Owing to this low lytic activity, it was not possible to establish if there is some kind of cooperativity in the dose–response curves. Also their lytic activities were too low to make them distinguishable. As a general tendency for both peptides in the interaction with anionic vesicles, the increase of negatively charged phospholipids enhanced the leakiness of the bilayers, with ANP-NH_2 being more lytic. This low leakage efficiency could not be attributed just to the peptides' chain length: another short-chain antimicrobial peptide studied in our laboratory [16], the less charged undecapeptide Decoralin (SLLSLIRKLIT) presents high permeabilizing efficiency in PCPG 7030 vesicles.

Planar Lipid Bilayer Preparation and Electrical Measurements

Considering that the poor permeability of CF, induced by ANP-NH_2 and ANP-OH in different vesicular bilayer compositions, could not explain their different antimicrobial action, the ion channel-like activity of these peptides has been investigated in azolectin planar lipid bilayers. Azolectin is a phospholipid extracted from soybeans with anionic character: its approximate composition is PC 23.5%, phosphatidylethanolamine (PE) 20%, inositol phosphatides 14%, other phospholipids, lipids and carbohydrates 39.5%. These characteristics make the bilayer features closer to PCCL 40:60 in relation to the contents in zwitterionic phospholipid.

Twenty to thirty minutes after the addition of the peptides to the *cis* compartment, ion channel-like activity was observed. Figure 2 shows representative recordings of ANP-NH_2 at clamping voltages of +100, +130, and +150 mV and of ANP-OH at +100 mV in azolectin bilayers. Under applied voltages, the activity of ANP-NH_2 was characterized by current fluctuations of similar amplitudes (unitary values) and occasionally, integer multiples of the unitary value. Figure 3 shows amplitude histograms of all events and dwell- time plots of ANP-NH_2 recordings. Histograms of all opening events indicate that unitary currents are distributed according to a normal Gaussian and dwell-time plots

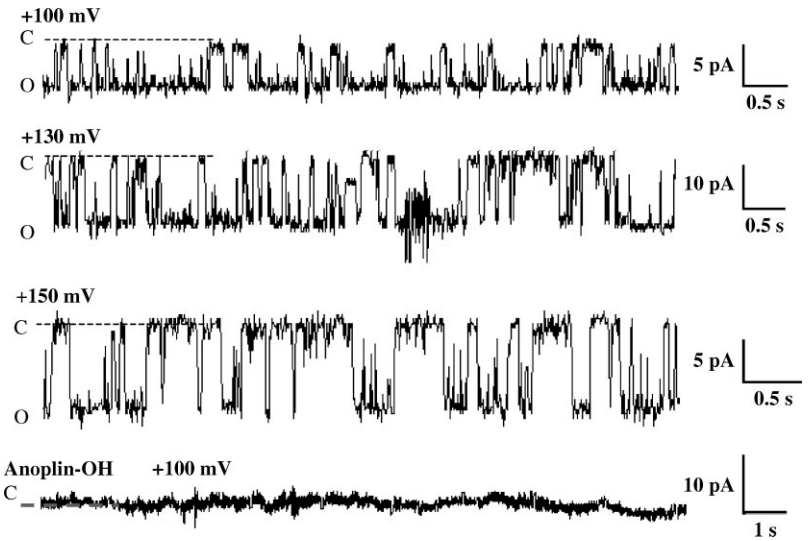

Figure 2 Single channel traces of ANP-NH_2 and ANP-OH. Representative recordings at different potentials, in azolectin bilayers. Aliquots of ANP-NH_2 (20 μl) or ANP-OH (25 μl) from stock solutions at 0.9 mM were added to the grounded *cis*-compartment containing 5 ml 10 mM Tris/HCl buffer with 150 mM KCl, pH 7.5, and different potentials were applied to the *trans*-side after stirring.

DOI: 10.1002/psc

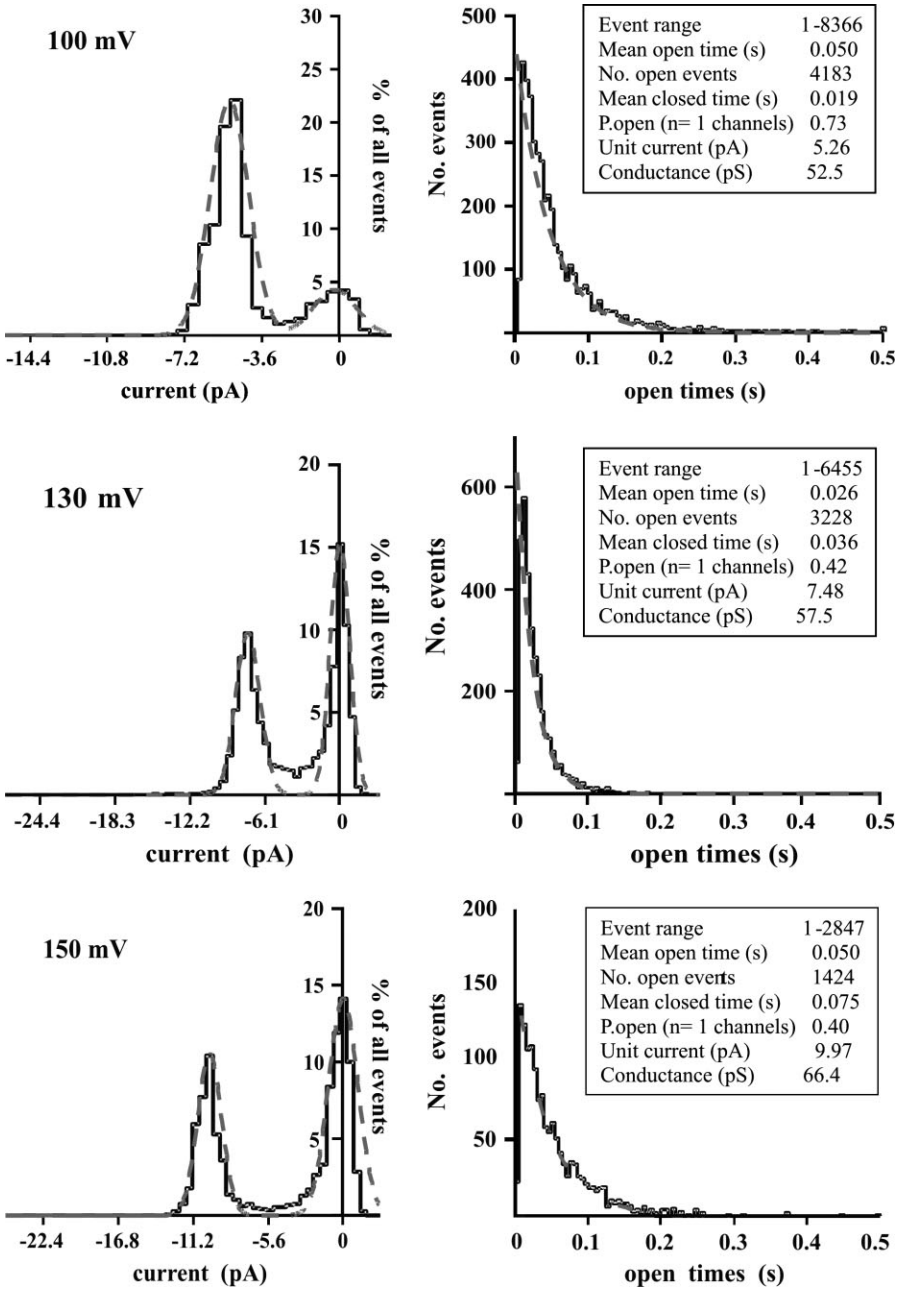

Figure 3 Statistical analysis of the entire single-channel recordings of ANP-NH2 in azolectin planar bilayers, corresponding to the traces shown in Figure 2. Histograms of current distributions of open events at different potentials, Gaussian-fitted, are shown in the left column; right column shows dwell-time plots fitted to exponential decays. The insert in the right column shows the number of events, the unit current and the conductance at each applied potential obtained from the histograms, and the mean open/closed times and the open probabilities from the lifetime distributions. The open probability, *P* open, is the ratio between the time during which the channel is open along the recording time.

of the open state conform to a mono-exponential distribution that assumed a two-state (open–closed) first-order kinetic model [12]. Average conductance is 50.7 ± 3.8 pS at 100 mV; 58.4 ± 2.7 pS at 130 mV; and 66.8 ± 6.7 pS at 150 mV. Mean open times ranged from 0.045 ± 0.006 s to 0.039 ± 0.016 s and open probabilities from 66 to 34% at, respectively, 100 and 150 mV. The ion channel-like activity of ANP-NH_2 has been detected at positive potentials as low as 15 mV, but only at 100 mV or higher it could be statistically analyzed.

Under negative voltage, single channels induced by ANP-NH_2 remain essentially open; there are small transitions that superimpose to this state, causing fluctuations around ± 5 pS in the bilayer conductance (data not shown). The average conductance in this state is approximately 46 pS. On the other hand, single-channel conductance measurements with ANP-OH

DOI: 10.1002/psc

showed only small and rare transitions with maximum bilayer conductance of 40 pS at 100 mV potential (Figure 2). At other potentials, either higher or lower, transitions are even rarer and insignificant.

ANP-NH_2 forms channels or pores whose cation-to-anion selectivity has been investigated. Under current-clamp, the system voltage recorded immediately after membrane breaking was approximately half of the total voltage measured before breaking the membrane. This indicates that the membrane voltage follows a Nernst potential as a function of the K^+ concentration in the *cis* side, and indicates 100% selectivity for cations, that is, 100% selectivity of K^+ over Cl^-.

Assuming cylindrical pore geometry and a membrane thickness of 3 nm, the diameter of a pore was estimated to be 0.5–0.6 nm, by comparing the measured pore conductance with that of an aqueous cylinder with the same electrolytic composition (150 mM KCl). For this, we considered that the only mobile species was K^+. A pore of this diameter explains why leakage was hardly observed, since CF is a molecule of about 1 nm diameter.

CD Spectroscopy Experiments

The secondary structure of ANP-NH_2 has been previously investigated employing CD spectroscopy [1,3]. Similarly, the CD spectra of ANP-OH (Figure 4) show random-coil features in Tris buffer and helical features in amphipathic environments, although the characteristic double minima at 208 and 222 nm are slightly displaced. Its molar ellipticity is around 30% smaller in 40% TFE/buffer mixture and around 20% smaller in buffered 8 mM SDS solution in relation to ANP-NH_2. Fitting of spectra with CDPro (CONTIN, SMP56) programs indicated 28–29% unordered structures for both peptides, 32–43% helical structures (regular and distorted), and 17–21% turns, with minimal differences between both peptides.

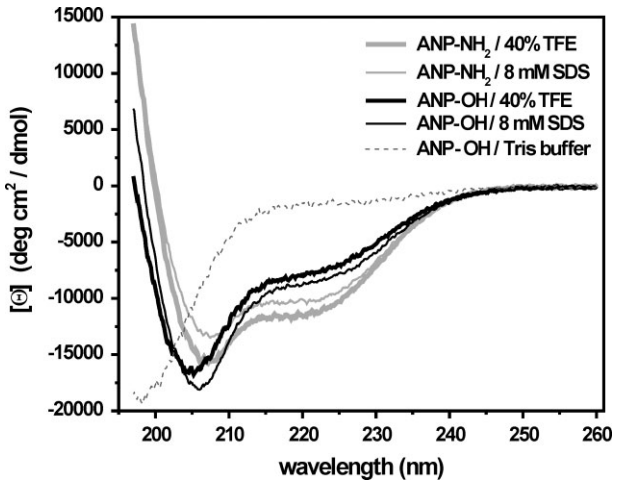

Figure 4 CD spectra of ANP-NH2 and ANP-OH at 20 μM, 25 °C. Amphipathic environments, like 40% TFE/water mixture or 8 mM SDS, induce α-helical secondary structures in comparison with Tris buffer, where peptides show unordered structures.

MD Simulations and Trajectory Analysis

Ion conductance through anionic membranes suggests that ANP-NH_2, but not ANP-OH, exerts its action by forming channel- or pore-like structures that might interfere with the ionic gradient of cells. The structural differences underlying the peptides' behavior in an amphipathic environment were investigated using MD simulations. CD and MD of antimicrobial peptides have extensively used TFE/water mixtures in structural investigations as a mimetic of the amphipathic environment of membranes [6,32,33]. Although it is an electrically neutral environment, it characterizes the tendency of the residues in a sequence to impose their preferences for the polar or apolar regions.

To prospect molecular differences between ANP-NH_2 and ANP-OH MD simulations were started from 100% ideal helix, since preliminary simulations showed that this procedure is more efficient at unraveling of the structure. Figure 5 shows the secondary structure per residue as a function of the simulation time for both peptides. This classification was obtained from the routines contained in Gromacs package [30]. For ANP-NH_2 (Figure 5(a)), the α-helix pattern is clearly obtained for almost all simulation times from residue 4 till residue 7. Residues 8 and 9 lose this conformation many times during very small time intervals. Residue 3 has a more constant dynamical behavior, but it remains out of this conformation for two periods of 1 ns each, performing 1/4 of the total running. The content of secondary structure for ANP-OH is lower than that of ANP-NH_2 as can be seen in Figure 5(b). Residues 3 to 6 are in α-helix while residue 8 seldom is and residue 9 is never in this conformation. Most of time, residue 7 is not in α-helix while residue 2 is in this conformation almost all time. These findings were confirmed following the trajectories of any (φ,ψ) peptidic dihedral angles (data not shown) and also through the calculation of the persistence of the H-bonds between the O (n) and N ($n+4$) that stabilize the α-helical structures.

Comparing the projected structures of ANP-NH_2 and ANP-OH (Figure 6), as obtained from the MD simulations, we found out that the polar face of ANP-OH is rather different because of the unfolding of a significant portion of the helical *C*-terminus, that moved residues Leu 9 and Leu 10 to the polar face of the peptide structure. ANP-OH has a negative charge at its *C*-terminus, which has been brought nearer the positive charges of the polar face; this means that ANP-OH shows a less amphipathic character than ANP-NH_2. No hydrogen bonding has been found among side chains of charged and polar residues and

DOI: 10.1002/psc

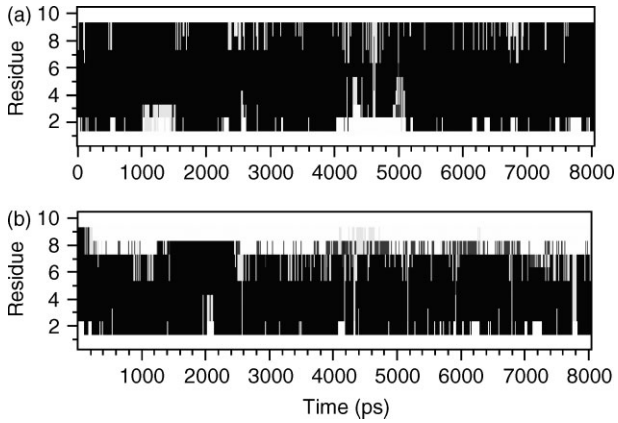

Figure 5 Secondary structure as a function of time for (a) ANP-NH2 and (b) ANP-OH. In black, residues in α-helix; gray, residues in turn or bend; white, residues in coil. It shows the deviation of each residue from the ideal helix.

amongst these residues and the backbone of both peptides, emphasizing the environment influence as the determinant of the secondary structure.

DISCUSSION

Amidation is one of the post-translational modifications that are associated with the resistance of the sequence to enzymatic degradation [4,20]. Amidation allows the accommodation of the *C*-terminus in an apolar environment, and it provides the possibility of an extra hydrogen bond within the α-helical structure [4,6]. Antimicrobial peptides with amidated *C*-terminus are ubiquitous [4,34] and, in many cases, amidation is associated with enhanced biological activities [4,5,20], although in other cases the opposite has been found [35]. According to the former cases, we found out that the synthetic deamidated analog of ANP lacks the characteristic antimicrobial and mast cell degranulating activities of the wild peptide. Although to a lesser extent than the amidated form, ANP-OH still retains the ability to fold into a helical structure when exposed to amphipathic environments such as TFE/water mixtures and anisotropic SDS micelles and anionic lipid bilayers [16], as determined in CD experiments. It has been observed for other peptides [5,11,36] that helical fraction and lytic activity on vesicles are well-correlated; with ANPs it has been observed that they are as poorly helical as lytic to vesicles. Other shortchain peptides derived from bovine lactoferricin, which adopt amphipathic structures but did not assume the α-helical or the β-sheet conformations, are also practically non-lytic to anionic vesicles [20].

The permeabilization of anionic and zwitterionic vesicles induced by ANP-NH_2 and ANP-OH at higher concentrations (20 μM) shows that pores or bilayer defects, large enough to leak just a small part of CF, are similarly formed, despite the peptides' structural differences. It also shows that leakage is dependent on the concurrence of a high peptide to lipid ratio. However, the investigation of the ion channel-like activity of ANPs confirms the ability of the amidated form, but not the carboxylated, to induce the formation of channel- or pore-like structures in anionic bilayers, at about the same concentration at which the antimicrobial activity has been observed. This fact is indicative of the formation of small pores or defects in vesicles, at lower peptide concentration, through which larger molecules about the size of CF are not able to leak, what makes the pore activity less detectable in this kind of experiment. Another important difference between the peptides' action on vesicles and planar bilayers concerns curvature: cationic peptides tend to induce positive curvature [37], which would add to the natural curvature strain imposed by lipids of the bilayer. The lytic activity of ANP-NH_2 and ANP-OH has been investigated in vesicles containing either PG or CL;

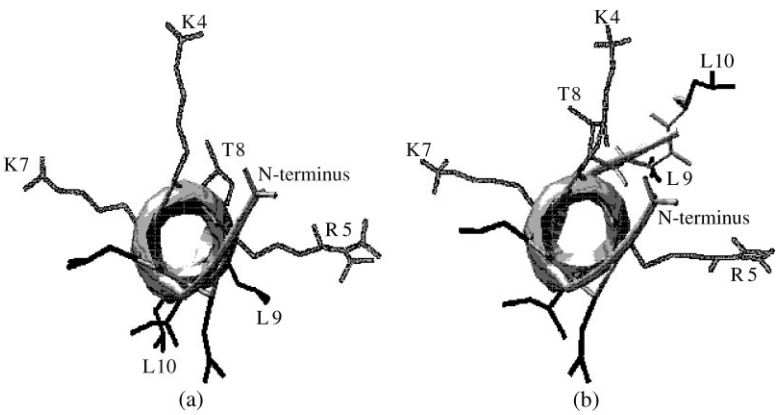

Figure 6 Helical projections of ANP-NH2 (panel a) and ANP-OH (panel b), as obtained from MD simulations in 30% TFE. They were projected on the normal plane to the helix axis, showing the polar angle between charged groups of Lys 7 and Arg 5. Side-chains of all hydrophobic residues, especially Leu 9 and Leu 10 are shown in black. Charged and polar residues are shown in dark gray.

DOI: 10.1002/psc

the former imposes positive curvature and the latter negative to the bilayer. From Figure 1, it can be seen that both forms of the peptide present more efficient permeabilization in the zwitterionic vesicles and the effect of lipids curvature could not be comparatively ascertained. Thus, planar bilayers made of azolectin, which are negatively charged, would be less favorable than the other vesicles concerning pore formation, as has been confirmed in the leakage experiment. Even though, the planar bilayer experiment shows the intense ANP-NH_2 activity.

MD simulations showed that the helical structure in ANP-NH_2 is maintained by a conjugation of the protection given to the main chain by an environment rich in hydrophobic CF_3, favoring the H-bonds and the repulsive interactions among the charged groups that apparently restrain the conformational space for the *N*-terminal. The presence of a negative charge at the *C*-terminus in ANP-OH introduces attractive interactions with cationic residues and shifts the apolar residue Leu 10 to the hydrophilic face of the helix. Coulombic forces dominate in low-dielectric environments [33] and the displacement of this *C*-terminus residue in ANP-OH to the polar side of the helix is well-correlated to its lower helical content as determined in CD experiments. Another consequence of this structural change is the decrease in the amphipathicity of the original chain, a physicochemical feature that has been often correlated with antimicrobial activity [7,20]. Like other wasp-venom peptides [11,17], the deamidation of ANP-NH_2 decreases or abolishes its mast cell degranulating activity, an unfavorable feature for an antibiotic agent. The changes in the biological activities of ANP-NH_2 due to carboxylation are related to electrostatic repulsion and lowering of its amphipathic character; these are important tools that can be used to modulate activity of short sequences, and whose effects can be evaluated by MD simulations.

We found out that ANP-NH_2 induces ion channels or pores in anionic bilayers, with a well-defined conductance step, and these pores remain open at *trans*-negative potentials; this situation is equivalent to the interaction of the peptide with bacterial membranes that also maintain a high negative potential inside [4,10]. At positive *trans*-potentials, the open channel probability dramatically decreases presenting a great number of transitions between open and closed states, and allowing statistical analysis to be performed. Nevertheless the transmembrane potential does not appear to be essential for the channel opening, since some leakage of fluorescent probes, like CF from vesicles, has been detected. Also, in planar bilayers, we found channel activity at close to zero voltages, but transmembrane potential is important for the intense pore activity.

The conductance of ANP pores, as measured in planar bilayers, varies between 50 to 70 pS, depending on the applied potential, showing a slight tendency to increase with voltages in the range of 100–150 mV. Open probabilities decrease from 66 to 34% in going from 100 to 150 mV, *trans*-side positive. However, the mean open time does not depend on the applied voltage, being about 40 ms. These data are indicative of the selective role of the transmembrane potential in bacteria, which could modify the open probability of an ion channel or pore. The conductance of ANP-NH_2 pores is compatible with that of an aqueous cylinder of 150 mM KCl, length 3 nm and a diameter of about 0.4 nm. Considering the selectivity to K^+ over Cl^-, this pushes the theoretical diameter to 0.5–0.6 nm, depending on the applied voltage. This estimate indicates a pore size with approximately half the size estimated for the pore of Mastoparan X, a tetradecapeptide, in PCPGPE (7 : 2 : 1) vesicle [38]. The ANP-NH_2 pore remains open at negative potentials, fluctuates between open and closed states at intermediary positive potentials and increases the tendency to the closed state at higher positive potentials.

Considering that ANP-NH_2 is just ten-residues long, made of bulky residues (average MW of side chains is 57.5 Da), with four positive charges, forms pores in the bilayer structure preferentially at negative potentials, does not show multiple discrete conductance levels, and conducts selectively K^+, through a 0.5–0.6 nm pore, there emerges a picture where the pore should be predominantly lined by negative charged molecules of lipids. This is consistent with a membrane toroidal defect, induced by the presence of destabilizing peptide molecules, whose inserted state is favored by negative potentials. A rough comparison with the pore features of magainin (23 residues long) raised some similarities as the bulkiness of residues, the number of positive charges, the absence of multiple discrete conductance levels, and the inside diameter [37]. Notwithstanding the reduced lytic activity of ANP-NH_2 in anionic vesicles, even at a concentration about 4 times that presenting antimicrobial activity [1], its activity on planar lipid bilayers is comparable to that of peptides whose mode of action supports the toroidal pore model [39].

Acknowledgements

M.P.S.C. has a post-doc (154550/2006-0) and M.A.-M. (142566/2005-5) has a doctorate fellowships from the Council for Scientific and Technological Development (CNPq); J.P. (301064/2004-0) and J.R.N. (310559/2006-5) are CNPq researchers, and S.T.B.C had CAPES doctorate fellowship.

REFERENCES

1. Konno K, Hisada M, Fontana R, Lorenzi CCB, Naoki H, Itagaki Y, Miwa A, Kawai N, Nakata Y, Yasuhara T, Ruggiero Neto J, Azevedo WF Jr, Palma MS, Nakajima T. Anoplin, a novel

antimicrobial peptide from the venom of the solitary wasp Anoplius samariensis. *Biochim. Biophys. Acta* 2001; **1550**: 70–80.
2. Eisenberg D, Schwarz E, Komaromy M, Wall R. Analysis of membrane and surface protein sequences with the hydrophobic moment plot. *J. Mol. Biol.* 1984; **179**: 125–142.
3. Ifrah D, Doisy X, Ryge TS, Hansen PR. Structure-activity relationship study of anoplin. *J. Pept. Sci.* 2005; **11**: 113–121.
4. Andreu D, Rivas L. Animal antimicrobial peptides: an overview. *Biopolymers* 1998; **47**: 415–433.
5. dos Santos Cabrera MP, de Souza BM, Fontana R, Konno K, Palma MS, de Azevedo WF Jr, Ruggiero Neto J. Conformation and lytic activity of eumenine mastoparan: a new antimicrobial peptide from wasp venom. *J. Pept. Res.* 2004; **64**: 95–103.
6. Sforça ML, Oyama S Jr, Canduri F, Lorenzi CCB, Pertinhez TA, Konno K, Souza BM, Palma MS, Ruggiero Neto J, de Azevedo WF Jr, Spisni A. How C-terminal carboxyamidation alters the biological activity of peptides from the venom of the eumenine solitary wasp. *Biochemistry* 2004; **43**: 5608–5617.
7. Dathe M, Meyer J, Beyermann M, Maul B, Hoischen C, Bienert M. General aspects of peptide selectivity towards lipid bilayers and cell membranes studied by variation of the structural parameters of amphipathic helical model peptides. *Biochim. Biophys. Acta* 2002; **1558**: 171–186.
8. Bechinger B, Lohner K. Detergent-like actions of linear amphipathic cationic antimicrobial peptides. *Biochim. Biophys. Acta* 2006; **1758**: 1529–1539.
9. Papo N, Shai Y. A molecular mechanism for lipopolysaccharide protection of Gram-negative bacteria from antimicrobial peptides. *J. Biol. Chem.* 2005; **280**: 10378–10387.
10. Zasloff M. Antimicrobial peptides of multicellular organisms. *Nature* 2002; **415**: 389–395.
11. Konno K, Hisada M, Naoki H, Itagaki Y, Fontana R, Rangel M, Oliveira JS, dos Santos Cabrera MP, Ruggiero Neto J, Hide I, Nakata Y, Yasuhara T, Nakajima T. Eumenitin, a novel antimicrobial peptide from the venom of the solitary eumenine wasp Eumenes rubronotatus. *Peptides* 2006; **27**: 2624–2631.
12. Hong H, Szabo G, Tamm LK. Electrostatic couplings in OmpA ion-channel gating suggest a mechanism for pore opening. *Nat. Chem. Biol.* 2006; **2**: 627–635.
13. Popplewell JF, Swann MJ, Freeman NJ, McDonnell C, Ford RC. Quantifying the effects of melittin on liposomes. *Biochim. Biophys. Acta* 2007; **1768**: 13–20.
14. Pearson WR, Lipman DJ. Improved tools for biological sequence comparison. *Proc. Natl. Acad. Sci. U.S.A.* 1988; **85**: 2444–2448, FASTA Copyright © 1988, 2006 by William R. Pearson and the University of Virginia.
15. Rogov VV, Lücke C, Muresanu L, Wienk H, Kleinhaus I, Werner K, Löhr F, Pristovsek P, Rüterjans H. Solution structure and stability of the full-length excisionase from bacteriophage HK022. *Eur. J. Biochem.* 2003; **270**: 4846–4858.
16. dos Santos Cabrera MP. Estudos da conformação e atividade lítica de peptídeos antimicrobianos de vespas. (PhD thesis in Molecular Biophysics) Instituto de Biociências, Letras e Ciências Exatas – IBILCE, UNESP-Universidade Estadual Paulista, São José do Rio Preto: Brasil, 2006.
17. Konno K, Hisada M, Naoki H, Itagaki Y, Kawai N, Miwa A, Yasuhara T, Morimoto Y, Nakata Y. Structure and biological activities of eumenine mastoparan-AF (EMP-AF), a new mast cell degranulating peptide in the venom of the solitary wasp (anterhynchium flavomarginatum micado). *Toxicon* 2000; **38**: 1505–1515.
18. Matsuzaki K. Why and how are peptide-lipid interactions utilized for self defense? *Biochem. Soc. Trans.* 2001; **29**: 598–601.
19. Yeaman MR, Yount NY. Mechanisms of antimicrobial peptide action and resistance. *Pharmacol. Ver.* 2003; **55**: 27–55.
20. Nguyen LT, Schibli DJ, Vogel HJ. Structural studies and model membrane interactions of two peptides derived from bovine lactoferricin. *J. Pept. Sci.* 2005; **11**: 379–389.
21. Allende D, McIntosh TJ. Lipopolysaccharides in bacterial membranes act like cholesterol in eukaryotic plasma membranes in providing protection against melittin-induced bilayer lysis. *Biochemistry* 2003; **42**: 1101–1108.
22. Mueller P, Rudin HT, Tien T, Wescott WC. Methods for the formation of single bimolecular lipid membranes in aqueous solutions. *J. Phys. Chem.* 1963; **67**: 534–535.
23. van Gunsteren WF, Billeter SR, Eising AA, Hünenberger PH, Krüger P, Mark AE, Scott WRP, Tironi IG. *Biomolecular Simulation: The GROMOS 96 Manual and User Guide; vdf Hochschulverlang.* ETH Zürich: Switzerland, 1996.
24. Berendsen HJC, Postma JPM, van Gunsteren WF, Hermans J. Interaction models for water in relation to protein hydration. In *Intermolecular Forces*, Pullman B. (ed.). Reidel Publishing Co: Dordrecht, The Netherlands, 1981; 331–342.
25. Fioroni M, Burger K, Mark AE, Roccatano D. A new 2,2,2-trifluoroethanol model for molecular dynamics simulations. *J. Phys. Chem. B* 2000; **104**: 12347–12354.
26. Hess B, Bekker H, Berendsen HJC, Fraaije JGE. LINCS: A linear constraint solver for molecular simulations. *J. Comput. Chem.* 1997; **18**: 1463–1472.
27. Miyamoto S, Kollman PA. SETTLE: An analytical version of the SHAKE and RATTLE algorithm for rigid water models. *J. Comput. Chem.* 1992; **13**: 952–962.
28. Berendsen HJC, Postma JPM, van Gunsteren W, Di Nola A, Haak JRJ. Molecular dynamics with coupling to an external bath. *J. Chem. Phys.* 1984; **81**: 3684–3690.
29. Cheatham TE III, Miller JL, Fox T, Darden TA, Kollman PA. Molecular dynamics simulations on solvated biomolecular system: The particle mesh Ewald method leads to stable trajectories of DNA, RNA, and proteins. *J. Am. Chem. Soc.* 1995; **117**: 4193–4194.
30. Lindahal E, Hess B, van der Spoel D. Gromacs 3.0: a package for molecular simulations and trajectory analysis. *J. Mol. Model.* 2001; **7**: 306–317.
31. Allende D, Simon SA, McIntosh TJ. Melittin-induced bilayer leakage depends on lipid material properties: evidence for toroidal pores. *Biophys. J.* 2005; **88**: 1828–1837.
32. Abbate S, Barlati S, Colombi M, Fornili SL, Francescato P, Gangemi F, Lebon F, Longhi G, Manitto P, Recca T, Speranza G, Zoppi N. Study of conformational properties of a biologically active peptide of fibronectin by circular dichroism, NMR and molecular dynamics simulation. *Phys. Chem. Chem. Phys.* 2006; **8**: 4668–4677.
33. Roccatano D, Colombo G, Fioroni M, Mark AE. Mechanism by which 2,2,2 trifluoroethanol/water mixtures stabilize secondary-structure formation in peptides: A molecular dynamics study. *Proc. Natl. Acad. Sci. U.S.A.* 2002; **99**: 12179–12184.
34. Tossi A, Sandri L, Giangaspero A. Amphipathic, α-helical antimicrobial peptides. *Biopolymers* 2000; **55**: 4–30.
35. Brogden KA, Ackermann M, McCray PB, Tack BF. Antimicrobial peptides in animals and their role in host defences. *Int. J. Antimicrob. Agents* 2003; **22**: 465–478.
36. Matsuzaki K, Sugishita K, Miyajima K. Interactions of an antimicrobial peptide, Magainin 2, with lipopolysaccharide-containing liposomes as a model for outer membranes of gram-negative bacteria. *FEBS Lett.* 1999; **449**: 221–224.
37. Matsuzaki K, Sugishita K, Ishibe N, Ueha M, Nakata S, Miyajima K, Epand RM. Relationship of membrane curvature to the formation of pores by magainin 2. *Biochemistry* 1998; **37**: 11856–11863.
38. Matsuzaki K, Yoneyama S, Murase O, Miyajima K. Transbilayer transport of ions and lipids coupled with mastoparan X translocation. *Biochemistry* 1996; **35**: 8450–8456.
39. Yang L, Harroun TA, Weiss TM, Ding L, Huang HW. Barrel-stave model or toroidal model? A case study on melittin pores. *Biophys. J.* 2001; **8**: 1475–1485.